This article has been accepted for publication in a future issue of this journal, but has not been fully edited. Content may change prior to final publication. Citation information: DOI 10.1109/TVT.2018.2805353, IEEE Transactions on Vehicular Technology

Hierarchical Energy Optimization Strategy and its Integrated Reliable Battery Fault Management for Hybrid Hydraulic-Electric Vehicle

Elkhatib Kamal and Lounis Adouane

***Abstract*—Reduction of fuel consumption is an indispensable part of automotive industry in recent years. This induces several developments of hybrid vehicles with different structures. This paper deals with reliable and robust energy management strategy for a hybrid hydraulic-electric intelligent vehicle. The main objective of this paper is the development of a suboptimal control strategy based on fuzzy logic and neural network for minimizing total energy consumption while ensuring a better battery life. For this purpose, fuzzy supervisory fault management, that can detect and compensate the battery faults, regulates all of the possible vehicle's operation modes. Then, control strategy based on fuzzy logic controller (FLC) is developed. The FLC membership function (MF) parameters are tuned by employing neural network to manage power distribution between electric motor and internal combustion engine (ICE). Control strategy is switched between optimized FLCs to enhance the suboptimal power split between the different energy sources and manage the ICE to work always in the vicinity of its optimal condition. Finally, a robust fuzzy tuning controllers are investigated to give a good torque set point tracking. Simulation results, while using TruckMaker/MATLAB software, confirm that the proposed approach leads to suboptimal energy consumption of the vehicle for any unknown driving cycles and compensate battery faults effects.**

***Index Terms*—Artificial intelligence; Battery management system; Fuzzy observer; Hybrid electric vehicles; Power management strategy; Sensor faults; Takagi-Sugeno fuzzy model.**

NOMENCLATURE

T_{ICE}, T_{HM}, T_{EM}: Produced torque for the Internal Combustion Engine (ICE), Hydraulic Motor (HM), Electric Motor (EM), respectively.
P_{ICE}, P_{HM}, P_{EM}: Produced power for the ICE, HM and EM, respectively.
$T_{ICE,SP}$, $T_{EM,SP}$: ICE and EM torque set point, respectively.
$\dot{m}_f$, ω_{EM}: Fuel flow rate of the ICE and EM current speed.
R_1, C_1: Activation polarization resistance and capacitance, respectively.
R_2, C_2: Concentration polarization resistance and capacitance, respectively.
R_o, T: Internal resistance and battery temperature, respectively.
V_{oc}: Battery open circuit voltage (OCV).
V_1, V_2: Voltages across R_1//C_1 and R_2//C_2.
T_{demand}: Torque demand.
δ_m: Current or voltage sensor measurement.
δ_m: Battery input current (I_{bat}) or terminal voltage (V_{bat}).
f_x: Current fault or voltage fault value.
$f_a(t)$, $f_s(t)$: Actuator faults and sensor faults respectively.
E_{si}, E_{ai}: Sensor and actuator fault matrices.
$x(t)$, $u(t)$, $y(t)$: State, control input and output vectors, respectively.
$\hat{X}(t)$, $\hat{Y}(t)$: Observer state, output vector, respectively.
$\hat{f}(t)$: Estimation of the sensor and actuator fault $f(t)$.
G_i, K_i and L_i: Controller and observer gains.
$\sigma_{ICE,j1}$ and $\sigma_{EM,i1}$, $\sigma_{ICE,j2}$ and $\sigma_{EM,i2}$: Mean and the standard deviation of the gaussian Membership Functions (MF) of the output variable for the ICE and the EM.
$m_{ICE,j}$ and $m_{EM,i}$: Inferred weights of the j^{th} and i^{th} output membership function for the ICE and the EM.

E. Kamal is with the Institut Pascal / Innovative Mobility: Smart and Sustainable Solutions (IMobS3), UCA/SIGMA UMR CNRS 6602, Clermont-Ferrand, France and also with the Department of Industrial Electronics and Control Engineering, Faculty of Electronic Engineering in Menouf, Menoufia University, Shebin EL Kom, Egypt (e-mail: elkateb.kamal@gmail.com).

L. Adouane is with the Institut Pascal / Innovative Mobility: Smart and Sustainable Solutions (IMobS3), UCA/SIGMA UMR CNRS 6602, Clermont-Ferrand, France (e-mail: Lounis Adouane@uca.fr).

This project is supported by the ADEME (Agence De l'Environnement et de la Maitrise de l'Energie) for the National French program Investissement d'Avenir, through BUSINOVA Evolution project, (see http://www.businova.com/en). This project received also the support of IMoBS3 Laboratory of Excellence (ANR-10-LABX-16-01).

I. INTRODUCTION

GROWING environmental concerns coupled to the decreasing of fossil fuel energy sources stimulate highly research on new vehicle technologies. Electric vehicles (EVs) and Hybrid Electric Vehicles (HEV) appears to be one of the most promising technologies for reducing fuel consumption and pollutant emissions [1]. Energy management in vehicles is an important issue because it can significantly influence the performances of the vehicles. Improving energy management in vehicles can deliver important benefits such as reducing fuel consumption, decreasing emission, lower running cost, reducing noise pollution, and improving driving performance and ease of use [2]. Several methods for energy management and optimization aiming at the minimization of different cost functions have been published [3]-[13], such as Dynamic Programming (DP) in [3] to formulate numerically a global optimum for reducing fuel consumption under the assumption of full knowledge of the future driving conditions. Unfortunately, the obtained results through DP cannot be implemented directly due to its high computational demands. To remedy this problem, approximated DP [4]

This article has been accepted for publication in a future issue of this journal, but has not been fully edited. Content may change prior to final publication. Citation information: DOI 10.1109/TVT.2018.2805353, IEEE Transactions on Vehicular Technology

and stochastic DP [5] had been suggested as possible solutions. Analytical optimization methods, on the other hand, use a mathematical problem formulation to find an analytical solution that makes the obtained solution faster than the purely numerical methods. Within this category, Pontryagin's minimum principle based energy management strategy is introduced as an optimal control solution [6]. This approach can only generate an optimal solution if implemented offline since in this case the future driving conditions are supposed to be known in prior. For online implementation rule based strategy from heuristic ideas have been proposed for HEVs [7] and a Hybrid Controller based on StateFlow (HCSF) is given in [8]. Fuzzy-based Blended Strategy (FBS) and rule-based is proposed in [9], [10]. Fuzzy Logic Controller (FLC) can imitate cognition and experience of human beings to depict the production process [11], and it can deal with imprecise information through linguistic expressions. In recent years, FLC has been successfully applied to numerous complicated issues that cannot be described with comprehensive mathematical model, but the rule based and database are often designed subjectively, which makes the logic rules and the membership functions cannot be adjusted adaptively [12]. As an optimized fuzzy control system, Genetic Algorithms (GA) and Genetic FLC (GFLC) has been applied to many fields and achieved remarkable results [13], [14]. However, the performance of GA has major impacts on the control effect of GFLC. Standard GA is most frequently faced with many drawbacks, such as premature convergence, local optimal deficiency, and no capacity of adaption [15]. To overcome time consumed by GA, Artificial Neural Network (ANN) is presented in [16], since ANN with Back Propagation (BP) learning algorithm is widely used in solving various classification and forecasting problems. Even though BP convergence is slow but it is generally guaranteed. However, very often ANN is considered as a black box learning approach, and cannot interpret immediate relationship between inputs and outputs mainly in presence of uncertainties. To overcome the drawbacks inherent to ANN, several approaches have been used in the literature [16], [17]. Among these approaches, fuzzy inference systems [10] are quite good in handling uncertainties and can interpret relationship between inputs/outputs by using appropriate rules. Therefore, to increase the capability of Fuzzy and ANN, hybridization of ANN and fuzzy is usually implemented [17]. One of the main objectives of this paper is the development and the validation of such control framework to minimize the energy consumption based on the merging of the two paradigms (ANN and Fuzzy system) to profit from their advantages and avoid their disadvantages.

Nowadays, there are different blending levels of pure EV and HEV available on the automotive industry. According to the blending level, various sizes, type and number of battery cells are mounted in HEVs and EVs [18]. Unlike conventional fuel, battery cells as an energy source have stricter requirements on their working environment [19]. The battery management system (BMS) is an essential emerging component of both EVs and HEVs alongside with modern power systems. Recently, Lithium-ion batteries can drastically improve the technical characteristics of EVs and HEV for various uses. However, Lithium-ion batteries require very special supervision. Hence, the need to integrate BMS as a supervision system becomes of great interest [20], [21]. The two main functions of the BMS are the State-Of-Charge (SOC) estimation, detect and diagnose the battery faults to prevent the battery from Over-Charge (OC) or Over-Discharge (OD). It is clear that the BMS operations highly depend on the installed sensors [22]. Therefore, the sensor faults detection and isolation (FDI) is of great importance to ensure the performance of the BMS. In addition, the battery sensor fault accelerate battery aging, decreasing thus its life and could cause also thermal runaway, which may cause fire and battery explosions.

Different approaches have been proposed to study battery faults [22]-[28]. Model based sensor using FDI scheme for a battery pack with a low computational effort is proposed in [22]. Model-based diagnostic scheme is presented in [23], it uses sliding mode observers designed according to the electrical and thermal dynamics of the battery. In [24] and [25], a systematic model-based FDI scheme is proposed for a Lithium-ion battery to detect and isolate the current, voltage and temperature sensor faults based on structural analysis theory. Detecting and diagnosing OC, OD faults in a Lithium-ion battery using nonlinear model representations are proposed in [26] and [27]. In [28], a robust Fault Tolerant Control (FTC) has been designed and implemented for a battery in order to minimize the energy consumption of autonomous vehicles while satisfying all production process-related constraints.

To implement the model-based fault diagnosis, a battery model is needed to capture the electrochemical properties [22]. Different battery models were studied by several researchers. The most commonly used models can be summarized as two kinds: the equivalent circuit models and the electrochemical models [29]-[37]. Recently, energy management optimization in consideration of battery life / degradation for HEV are studied in several works [38]-[43], in order to improve the total economy in driving process. According to the previous studies, a reliable battery fault tolerant control to guarantee the battery performance, safety and life while simultaneously minimizing the total energy consumption (summation of electric battery and fuel) for Hybrid Hydraulic-Electric Vehicles (HHEVs) are addressed in this paper. In order to study and develop an efficient and reliable energy management strategy for HHEV, a precise vehicle modelling is desirable based on [6], [36], [37]. The studied vehicle is a hybrid bus based on series-parallel power split hybrid architecture. This hybrid bus is called BUSINOVA and is developed by SAFRA Company (cf. Figure 1 and 2). BUSINOVA is composed of Electric Motor (EM), Internal Combustion Engine (ICE), Hydraulic Motor (HM), and battery as the propulsion powertrain system of the vehicle. The EM and HM motors are both directly connected to the transmission and can ensure simultaneously or independently the traction of the bus. On the other hand, the ICE is coupled to a Hydraulic Pump (HP) for driving the HM. This gives a large number of degrees of freedom for the

This article has been accepted for publication in a future issue of this journal, but has not been fully edited. Content may change prior to final publication. Citation information: DOI 10.1109/TVT.2018.2805353, IEEE Transactions on Vehicular Technology

bus, which increases the possible number of combinations of such degrees of freedom for energy optimization.

The main contributions of this paper is to propose and develop a fuzzy FTC for HHEVs battery to detect, isolate, and accommodate sensor faults. The Takagi-Sugeno (TS) fuzzy model is adopted for fuzzy modeling of the HHEV battery. The concept of parallel distributed compensation (PDC) is employed to design fuzzy control from the TS fuzzy models. Sufficient conditions are formulated in the format of linear matrix inequalities (LMIs).

In addition, minimize the total energy consumption in order to enhance the bus energy efficiency is proposed. It is based on Intelligent Robust Hierarchical Hybrid Controller Strategy (IRHHCS cf. Section III). The proposed IRHHCS consists of three control levels based on neural network, fuzzy logic and rules based optimization. An Intelligent Supervisory Switching Mode and Battery Management Controller (ISSMBMC) based on fuzzy logic is developed in the third level (the highest level) that is capable of managing all of the possible bus operation modes, compensate the battery faults, generating suboptimal mode and SOC set points for second level. In the second level, a Robust Energy Management Controller (REMS) is proposed. It is based on neural fuzzy logic control to manage and optimize the power distribution between the two different sources. Then, in the first level (the lowest one), there are Subsystem Robust Fuzzy Tuning Controllers (SRFTC) to regulate the set points of each vehicle sub-systems (EM, battery, ICE, HP and HM) to achieve the best operational performance. The proposed strategy is compared to HCSF [8] and FBS [10], to illustrate the effectiveness of the proposed control technique (cf. Section IV).

The proposed strategy leads to have several main advantages, among them let us cite: (i) it can be easily implemented in real time and can be used by various structures of hybrid vehicles; (ii) it can reduce, while using appropriate optimization strategy, the total energy consumption (compared to other strategies); (iii) it can detect, isolate and compensate the battery voltage sensor faults and battery current actuator faults; (iv) it does not depend on the a-priori knowledge of the driving event, which making it suitable to be implemented online.

The paper is organized as follows. Section II will present the studied vehicle which corresponds to BUSINOVA bus. The analyse of the proposed control strategy of the vehicle is given in section III. Section IV shows the experiment model validation, fault effects analysis and validate the proposed strategy over different drive cycles (European standard New European Driving Cycles (NEDC) and the Urban Dynamometer Driving Schedule (UDDS) long cycle). Section V is devoted to give a conclusion and some prospects.

II. Overall HHEV Modeling and Description

This section presents modelling and analysis of the studied HHEV based on [6], [36], [37] with its different operations modes. TruckMaker/MATLAB software is used to simulate precisely the studied hybrid vehicle.

A. HHEV Description and Modelling

The studied vehicle corresponds to BUSINOVA bus shown in Figure 1. The parameters used for the vehicle modeling is presented in the Table III of the appendix A. This bus has three actuations: electric, hydraulic and thermal. The principle source of the propulsion in the vehicle is an EM which may be supplemented by the HM via ICE. The hydraulic system block consists of variable-displacement of HM, and an ICE driven fixed-displacement of HP. The ICE is directly connected to a fixed displacement pump, which converts engine mechanical power into hydraulic power as shown in the vehicle configuration and power flow diagram (cf. Figure 2). The BUSINOVA is equipped with electric, hydrostatic and dissipative braking capabilities. The dissipative brake is a mechanical brake which dissipates energy as heat through friction. Electric and hydrostatic brakes are linked to the hydraulic motor in a regenerative braking system that is capable of recovering a portion of the kinetic energy of braking that would otherwise be dissipated. An Electrical Junction (EJ) exists between the battery, accessories (Access) and dual converter as well as a Mechanical Junction (MJ) between the HM and EM.

Fig. 1. BUSINOVA an Hybrid Hydraulic-Electric bus.

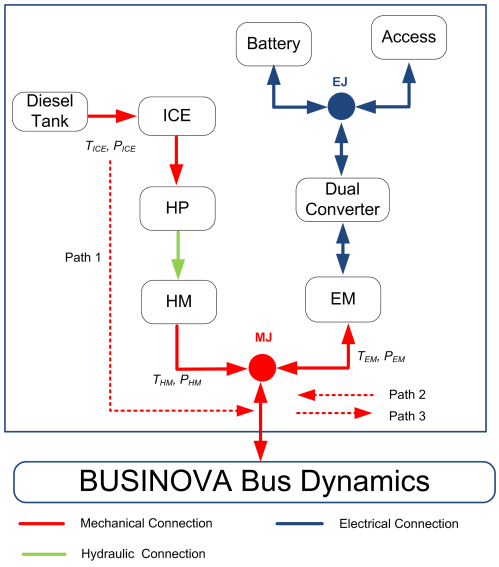

Fig. 2. BUSINOVA bus configuration and power flow. T_{ICE}, T_{HM}, T_{EM} and P_{ICE}, P_{HM}, P_{EM} are the produced torque and power for the ICE, HM and EM, respectively.

This article has been accepted for publication in a future issue of this journal, but has not been fully edited. Content may change prior to final publication. Citation information: DOI 10.1109/TVT.2018.2805353, IEEE Transactions on Vehicular Technology

B. Motoring Models

HM model through ICE and the EM models based on [6] are given in this section as the following.

1) Hydraulic Motor Coupled to Internal Combustion gine: In this paper, ICE torque versus ICE speed is dir derived from the ICE fuel consumption model. The fuel rate $\dot{m}_f$ of the ICE is defined by

$$\dot{m}_f = f_{ICE}(T_{ICE}, \omega_{ICE})$$

where ω_{ICE} is the ICE rotational speed. The function f is obtained from the ICE bench tests. The power consu by the ICE (P_{ICE}) is given by P_{ICE}=$\dot{m}_f(T_{ICE}, \omega_{ICE})Q$ (i.e., P_{ICE} is the instantaneous power of the fuel expre in terms of $\dot{m}_f$ and the lower heating value of the fuel (Q = 43 MJ/Kg). Figure 3(left) shows the relationship between HM speed, HM torque and HM consumed power. Developing an accurate fuel consumption model is very important for addressing energy consumption optimization problems. The specification parameters of the ICE, hydraulic motor and pump are given respectively in the Tables IV and V (cf. Appendix A).

2) Electric Motor: The studied hybrid bus uses a 103 KW permanent magnet synchronous machine as EM. The powers required for the EM were calculated from the known EM torque and speed by using EM efficiency curve as shown in Figure 3 (right). The output torque T_{EM} of the EM is defined by

$$T_{EM} = f_{EM}(P_{EM}, \omega_{EM}) \tag{2}$$

where P_{EM} is the EM input power, ω_{EM} is the EM current speed. The function f_{EM} is also obtained from the EM bench test. The EM can operate in motor or generator mode. In generator mode, the electric motor converts the kinetic energy from vehicle regenerative braking into electrical energy stored in the battery. In the motor mode, the electric motor converts electrical energy into kinetic energy to move the vehicle. The main parameters of the traction electric motor used in BUSINOVA are presented in the Table VI (cf. Appendix A). The efficiency characteristics data of the EM, and HM coupled to the ICE given in Figure 3 are implemented in IPG automotive TruckMaker software.

C. BUSINOVA Lithium-ion Battery Modeling

The battery model is necessary for its SOC estimation. Different Lithium-ion battery models are developed in the literatures [29]-[37]. The equivalent electrical circuit models and the electrochemical models are the most widely used in EV studies. The electrical circuit models use equivalent electrical circuits to show current-voltage characteristics of batteries by using voltage and current sources, capacitors, and resistors. For the BUSINOVA bus battery, its model is based on [36], [37] (cf. Figure 4). The electrical behavior of the practical model can be expressed as follows:

$$V_{bat} = V_{oc} - I_{bat}R_o - V_1(t) - V_2(t) \tag{3}$$

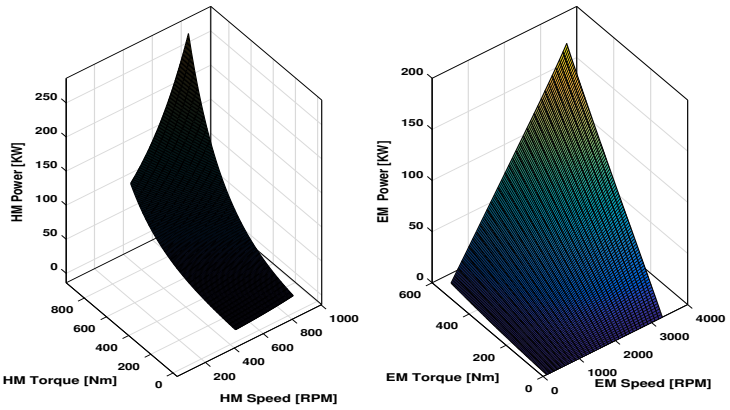

Fig. 3. Power consumption mapping; (left) efficiency characteristics of the HM coupled to ICE; (right) efficiency characteristics of the EM.

where V_{bat} is the battery terminal voltage, V_{oc} is the battery open circuit voltage (OCV), I_{bat} is the battery input current, t is the time varying, V_1, V_2 are the voltages across R_1//C_1 and R_2//C_2, where R_1 and C_1 are the electrochemical polarization resistance, capacitance, respectively, R_2 and C_2 are the concentration polarization resistance, capacitance, respectively and R_o is the internal resistance which consists to the bulk resistance and surface layer impedance. The BUSINOVA bus battery parameters are presented in the Table VII in the Appendix A. Using Kirchhoff's voltage law, the voltage across capacitor C_1 is given by

$$\dot{V}_1(t) = -\frac{V_1(t)}{R_1C_1} + \frac{I_{bat}}{C_1} \tag{4}$$

The voltage across capacitor C_2 is given by

$$\dot{V}_2(t) = -\frac{V_2(t)}{R_2C_2} + \frac{I_{bat}}{C_2} \tag{5}$$

The SOC is the ratio of the remaining capacity to the nominal capacity of the battery cell and is given by [36]-[44]

$$SOC = SOC_i + \frac{\int \eta_{co} I_{bat} dt}{C_n} \tag{6}$$

where SOC$_i$ is the initial value of the SOC, C_n is the nominal capacity in Ampere-hours ($A-h$) and η_{co} is the Coulombic efficiency. The tested cells are done always between 10% and 95% of the SOC, which corresponds to the imposed operational work of the bus. In addition, V_1 and V_2 are assumed to be not zero conditions. The derivative of SOC in (6) is given by,

$$\dot{SOC} = \frac{\eta_{co} I_{bat}}{C_n} \tag{7}$$

From (4), (5) and (7), the dynamics of the nonlinear battery behavior can be characterized by the following equations,

$$\begin{aligned} \dot{x}(t) &= Ax(t) + Bu(t) \\ y(t) &= C(x)x(t) \end{aligned} \tag{8}$$

This article has been accepted for publication in a future issue of this journal, but has not been fully edited. Content may change prior to final publication. Citation information: DOI 10.1109/TVT.2018.2805353, IEEE Transactions on Vehicular Technology

where $x(t) = \begin{bmatrix} V_1(t) \\ V_2(t) \\ SOC \end{bmatrix}$, $A = \begin{bmatrix} -\frac{1}{R_1 C_1} & 0 & 0 \\ 0 & -\frac{1}{R_2 C_2} & 0 \\ 0 & 0 & 0 \end{bmatrix}$, $B = \begin{bmatrix} \frac{1}{C_1} \\ \frac{1}{C_2} \\ \frac{\eta_{co}}{C_n} \end{bmatrix}$, $C(x) = \begin{bmatrix} q_1(x) \\ 1 \\ q_2(x) \end{bmatrix}^T$, $u(t) = I_{bat}$ and $y(t) = V_{bat}$ where $q_1(x) = \frac{(I_{bat} R_o + V_1(t))}{V_1(t)}$ and $q_2(x) = \frac{V_{oc}}{SOC}$. Due to the nonlinearity in V_{oc}, the output of the battery system is nonlinear.

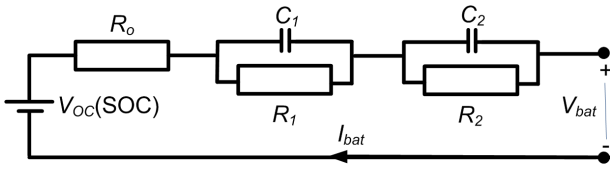

Fig. 4. BUSINOVA Lithium-ion battery equivalent electrical model.

D. HHEV Torque Distribution and Operation Modes

During the bus displacement, its suboptimal control depends on the accurate knowledge of torque required to propel the bus and charge the battery. One of the objective of the control strategy is to split the total torque between the HM via ICE and EM to optimize the efficiency of the main components (cf. Section III.B). Figure 2 shows the torque paths between HM via ICE and the EM as the following:

- Path 1: HM drives the wheels via the ICE.
- Path 2: EM used as a motor to drive the wheels.
- Path 3: EM is used as a generator to charge the battery.

Due to the nature of HHEV and depending on the torque distribution, there are five possible modes of operation:

- EM Mode: EM only (path 2).
- ICE Mode: HM via ICE only (path 1).
- Hybrid Mode: EM assisted by HM via ICE (path 1 and 2).
- Charging Mode (CM): Battery charging by ICE(path 1 and 3).
- Regenerative Braking Mode (RBM): Battery charging by regenerative braking Energy (path 3).

As far as possible, each component of the TruckMaker simulator should correspond to an actual component on the HHEVs. Table III to Table VII in the appendix A indicate the specification of the studied HHEV.

III. Proposed Intelligent Robust Hierarchical Hybrid Controller Strategy (IRHHCS)

In this section, the control strategy is developed for power control, torque splitting between EM and ICE and to detect and compensate the battery faults. The proposed IRHHCS structure consists of three control levels (cf. Figure 5). In this figure the following acronyms are used: VECP is the vehicle energy consumed and produced), AVT is the actual vehicle torque and T_{demand} is the torque demand. The third level has been developed by fuzzy strategy and fuzzy observer wwhich decides the operating mode or combination of modes which would be the most efficient based on a healthy SOC (cf. Section III.A). This level consists of two blocks, the first block corresponds to a Battery Management Fuzzy Fault Tolerant Controller (BMFFTC) to detect and compensate the battery faults and generate the healthy SOC (the healthy SOC means SOC value determination without faults) for the Fuzzy Switching Mode Controller (FSMC) which selects the optimal mode for the second level. A Robust Energy Management Controller (REMS) has been designed in the second level (cf. Section III.B) to manage power distribution between EM and ICE and minimizing fuel consumption. In the first level, Subsystem Robust Fuzzy Tuning Controllers (SRFTC) is described and used to track the set points of EM and HM via the ICE (generated at the second level), in order to reach peak performance and acceptable operation indices while taking into consideration of the dynamic behavior of EM, ICE and HM. The proposed strategy can be used for both offline and online scenarios. Offline scenario implies that the information about the future driving cycle and the environment (road profile, vehicle weight, etc.) are fully known, whereas for the online scenarios this information is obtained in real time.

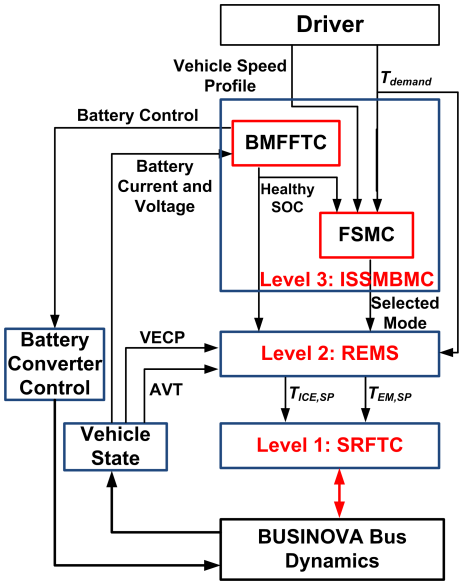

Fig. 5. Proposed IRHHCS for BUSINOVA bus.

A. Intelligent Supervisory Switching Mode and Battery management Controller (Level 3: ISSMBMC)

The objective of this section is to optimize the selection mode, and detect and compensate the battery sensor faults (battery terminal voltage sensor) and the actuator faults (battery input current actuator). This level consists of BMFFTC and FSMC blocks to generate the selected mode and the SOC set point for the second level. Figure 6 shows the block diagram of the proposed level 3.

1) Fuzzy Switching Mode Controller (FSMC): Intelligent fuzzy supervisory switching mode controller has been developed in this paper. This controller contains three input variables and one output variable. It is assumed that the ICE

This article has been accepted for publication in a future issue of this journal, but has not been fully edited. Content may change prior to final publication. Citation information: DOI 10.1109/TVT.2018.2805353, IEEE Transactions on Vehicular Technology

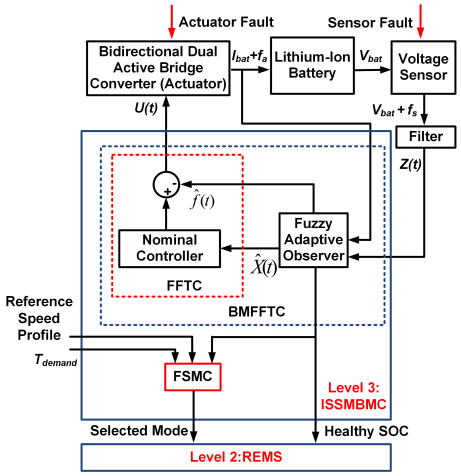

Fig. 6. Schematic of the proposed level 3.

will recharge the battery. The input variables for the FSMC are the velocity of the vehicle, T_{demand} and SOC. The output variable is Operation Mode (OM). Fuzzy rule base in the case of regenerative braking and charging mode of the FSMC are shown in Table I. Where L is the low, M is the medium and M is the high. Gaussian Membership Functions (MF) and Center of Gravity (COG) defuzzification are used.

TABLE I
FUZZY RULE BASE IN THE CASE OF REGENERATIVE BRAKING AND CHARGING MODE

SOC	T_{demand}	Speed	OM
L or M or H	Braking	L or M or H	RBM
L or M	Acclerating	L or M or H	CM
L or M	very Acclerating	L or M or H	CM

2) Battery Management Fuzzy Fault Tolerant Controller (BMFFTC): The main objective for the BMFFTC is to mange and control the battery faults and to generate the healthy SOC set point for FSMC and the second level which affects the studied HHEV power optimization. The general configuration of BMFFTC is given in Figure 6. This section presents a systematic fault diagnosis and control scheme for the battery cell to detect current and/or voltage sensor faults, and compensate their effects. For the diagnostic and control scheme implementation, new Fuzzy Fault Tolerant Control (FFTC) based on fuzzy adaptive observer is proposed to estimate and compensate the effect of the battery faults (current sensor faults, and/ or voltage sensor faults). The concept of PDC (Parallel Distributed Compensation) [44] is employed to design fuzzy control and fuzzy adaptive observer from the TS fuzzy models. Sufficient conditions are derived for robust stabilization in the sense of Lyapunov stability, for voltage sensor faults, current actuator faults and state variables unavailable for measurements. The sufficient conditions are formulated in the format of LMI (Linear Matrix Inequalities). In this paper, we consider that the sensor faults can occur at the same time or only one sensor fault at a time. Most of the HEV battery sensors (for measuring currents and voltages) use Hall effect and they are generally subject to bias (offset) and gain fault (scaling) [45]. Bias fault is a constant offset from the nominal statistics of the sensor signal, while gain fault is a time-varying offset. The bias and gain faults are considered additive faults in industrial applications [46] and they are modeled as the following.

$$\delta_m = \delta + E_x f_x(t) \tag{9}$$

where δ_m is the current or voltage sensor measurement, δ is the battery input current (I_{bat}) or terminal voltage (V_{bat}), f_x is the fault value and E_x is the fault matrix. In order to design the BMFFTC, we need to represent the battery model based on TS fuzzy model, design fault estimation based on the fuzzy adaptive observer and design FFTC as the following.

a) Takagi-Sugeno's Fuzzy Battery Model with Faults: Consider the i^{th} rule of the TS fuzzy model expressed in the following If-Then rules [44].

$$\begin{aligned} \text{Plant Rule } i\text{: If } & q_1(t) \text{ is } h_{i1} \text{ and} \dots \text{and } q_\psi(t) \text{ is } h_{i\psi}(t) \\ \text{Then } & \dot{x}(t) = A_i x(t) + B_i u(t) + E_{ai} f_a(t) \\ & y(t) = C_i x(t) + E_{si} f_s(t) \end{aligned} \tag{10}$$

where $x(t)$ is the state vector, $u(t)$ is the control input vector, $y(t)$ is the output vector, $(j = 1, 2, \dots, \psi)$ and h_{ij} $(i = 1, 2, \dots, p; j = 1, 2, \dots, \psi)$ are the premise variable and the fuzzy sets that are characterized by the membership function, ψ is the number of the premise variable, p is the number of rules of the TS fuzzy model, $A_i \in \Re^{n\times n}$, $B_i \in \Re^{n\times m}$ and $C_i \in \Re^{g\times n}$ are system, input and output matrices, respectively, $f_a(t)$, $f_s(t)$ are the actuator faults, sensor faults, E_{si} is the sensor fault matrix, E_{ai} is the actuator fault matrix and $q_1(t)$,..., $q_\psi(t)$ are assumed measurable variables and do not depend on the sensor faults and the actuator faults. The overall fuzzy model achieved by fuzzy blending of each individual plant rule is given by,

$$\begin{aligned} \dot{x}(t) &= \sum_{i=1}^{p} \mu_i(q(t))[A_i x(t) + B_i u(t) + E_{ai} f_a(t)] \\ y(t) &= \sum_{i=1}^{p} \mu_i(q(t))[C_i x(t) + E_{si} f_s(t)] \end{aligned} \tag{11}$$

where $Q_i(q(t)) = \prod_{j=1}^{\psi} h_{ij}(q_j(t))$, $\mu_i(q(t)) = \frac{Q_i(q(t))}{\sum_{i=1}^{p} Q_i(q(t))}$ in which $h_{ij}(q_j(t))$ is the grade of membership of $q_j(t)$ in h_{ij}. Some basic properties of $Q_i(q(t))$ are given by, $Q_i(q(t)) \geq 0$, $\sum_{i=1}^{p} Q_i(q(t)) > 0$, $i = 1, 2, \dots, p$. It is known that $\mu_i(q(t)) \geq 0$, $\sum_{i=1}^{p} \mu_i(q(t)) = 1$, writing $\mu_i(q(t))$ as μ_i for simplicity. Considering also the state $Z \in \Re^{g\times 1}$ that is a filtered version of the output $y(t)$ [47]. This state is given by:

$$\dot{Z}(t) = \sum_{i=1}^{p} \mu_i[-A_{zi} Z(t) + A_{zi} C_i x(t) + A_{zi} E_{si} f_s(t)] \tag{12}$$

where $-A_{zi} \in \Re^{r\times r}$ is the stable matrix, from (11) and (12), one can obtain the augmented system:

$$\begin{aligned} \dot{X}(t) &= \sum_{i=1}^{p} \mu_i[\bar{A}_i X(t) + \bar{B}_i U(t) + \bar{E}_i f(t)] \\ Y(t) &= \sum_{i=1}^{p} \mu_i \bar{C}_i X(t) \end{aligned} \tag{13}$$

This article has been accepted for publication in a future issue of this journal, but has not been fully edited. Content may change prior to final publication. Citation information: DOI 10.1109/TVT.2018.2805353, IEEE Transactions on Vehicular Technology

where $X(t)=\begin{bmatrix}x(t)\\Z(t)\end{bmatrix}$, $U(t)=\begin{bmatrix}u(t)\\0\end{bmatrix}$, $f(t)=\begin{bmatrix}f_a(t)\\f_s(t)\end{bmatrix}$, $\bar{A}_i=\begin{bmatrix}A_i & 0\\A_{zi}C_i & -A_{zi}\end{bmatrix}$, $\bar{B}_i=\begin{bmatrix}B_i & 0\\0 & 0\end{bmatrix}$, $\bar{E}_i=\begin{bmatrix}E_{ai} & 0\\0 & A_{zi}E_{si}\end{bmatrix}$ and $\bar{C}_i=\begin{bmatrix}0 & I\end{bmatrix}$.

b) Fuzzy Adaptive Observer: In order to estimate the state and the fault of the battery (8), the following fuzzy adaptive observer is proposed based on [48],

$$\dot{\hat{X}}(t)=\sum_{i=1}^{p}\mu_i[\bar{A}_i\hat{X}(t)+\bar{B}_iU(t)+\hat{E}_i\hat{f}(t)+K_i(Y(t)-\hat{Y}(t))] \quad (14)$$

$$e_x(t)=X(t)-\hat{X}(t) \quad (15)$$

$$e_y(t)=Y(t)-\hat{Y}(t)=\bar{C}_ie_x(t) \quad (16)$$

$$\dot{\hat{f}}(t)=\sum_{i=1}^{p}\mu_iL_i(\dot{e}_y(t)+e_y(t))=\sum_{i=1}^{p}\mu_iL_i\bar{C}_i(\dot{e}_x(t)+e_x(t)) \quad (17)$$

$$\hat{Y}(t)=\sum_{i=1}^{p}\mu_i\bar{C}_i\hat{X}(t) \quad (18)$$

where $\hat{X}(t)$ is the observer state, $\hat{Y}(t)$ is the observer output vector, $\hat{f}(t)$ is an estimation of the sensor and actuator fault $f(t)$, K_i and L_i are the observer gains to be designed.

c) Proposed Fuzzy Fault Tolerant Control: In this section, the FFTC synthesis procedure is developed to deal with a wide range of sensor faults, and actuator faults while maintaining the stability of the closed loop battery system. For simplicity, we make $\bar{E}_j=\bar{B}_jE_j$, where, E_j are known matrix. For the fuzzy model (11), we construct the following FFTC via the PDC [44]. It is assumed that the fuzzy system (11) is locally controllable. A state-feedback with LMIs is used to design a controller for each subsystem. The final output of the FFTC based on online fault estimation is defined and is based on [48],

$$U(t)=\sum_{j=1}^{p}\mu_j[G_j\hat{X}(t)-E_j\hat{f}(t)] \quad (19)$$

where, G_i are the controller gain to be designed, the sensor and the actuator fault vectors are assumed to be bounded. The main result for the global asymptotic stability of a TS fuzzy model with sensor and actuator faults are summarized by the following Theorem 1.

Theorem 1: The TS fuzzy system (13) is asymptotically stabilizable if there exist symmetric and positive definite matrix *P (P>0)*, some matrices L_i, K_i, and G_j *(i=1,2,…,p; j=1,2,…,q)*, such that the following LMIs are satisfied,

$$O\,A_i^T+A_iO-(B_i\,W_j)^T-(B_i\,W_j)<0 \quad (20)$$

$$H_{bi}^T\,P_2+P_2\,H_{bi}-(D_i\,C_i)^T-(D_i\,C_i)<0 \quad (21)$$

where $P=diag(P_1,P_2)$, $O=P_1^{-1}$, $G_j=W_jO^{-1}$, $\bar{K}_i$=$P_2^{-1}D_i$, $\bar{K}_i=\begin{bmatrix}K_i\\L_i\end{bmatrix}$.

Proof. The conditions imposed to develop the theorem is shown in the Appendix B.

d) BUSINOVA Lithium-ion Battery Model Based on TS Fuzzy Model: To design the FFTC and the fuzzy adaptive Observer, a fuzzy model that represents the dynamics of the battery is necessary. Therefore, the system is first represented with a TS fuzzy model. The system (8) is described by a TS fuzzy representation. Next, calculate the minimum and maximum values of $q_1(x)$ and $q_2(x)$ under the constraints $q_{1,min}\le q_1(x)\le q_{1,max}$ and $q_{2,min}\le q_2(x)\le q_{2,max}$. From the maximum and minimum values $q_1(x)$ and $q_2(x)$, one can obtain the nonlinearity sector as follows

$$\begin{aligned}q_1(x)&=q_{1,max}N_1(q_1(x))+q_{1,min}N_2(q_1(x))\\q_2(x)&=q_{2,max}M_1(q_2(x))+q_{2,min}M_2(q_2(x))\end{aligned} \quad (22)$$

where $N_1(q_1(x))+N_2(q_1(x))=1$, $M_1(q_1(x))+M_2(q_1(x))=1$ (as commonly used in the literature [44], [48]), N_{i1} and M_{i2} are a fuzzy term of rule i, $q_1(x)$ and $q_2(x)$ are the premise variables. Then, the nonlinear battery is represented by the following fuzzy model.

Plant Rule *i*: If $q_1(x)$ is N_{i1} and $q_2(x)$ is M_{i1}
Then $\dot{x}(t)=A_ix(t)+B_iu(t)+E_{ai}f_a(t)$
$y(t)=C_ix(t)+E_{si}f_s(t),\quad i=1,\dots,4.$ (23)

Referring to (10), the fuzzy plant model given by

$$\begin{aligned}\dot{x}(t)&=\sum_{i=1}^{4}\mu_i[A_ix(t)+B_iu(t)+E_{ai}f_a(t)]\\y(t)&=\sum_{i=1}^{4}\mu_i[C_ix(t)+E_{si}f_s(t)]\end{aligned} \quad (24)$$

where $x(t)\in\Re^{3\times1}$, $u(t)\in\Re^{1\times1}$ and $C_i\in\Re^{1\times3}$ are the state vectors and the battery control input, respectively, where $A_1=A_2=A_3=A_4=\begin{bmatrix}-\frac{1}{R_1C_1} & 0 & 0\\0 & -\frac{1}{R_2C_2} & 0\\0 & 0 & 0\end{bmatrix}$, $B_1=B_2=B_3=B_4=\begin{bmatrix}\frac{1}{C_1}\\\frac{1}{C_2}\\\frac{\eta_{co}}{C_n}\end{bmatrix}$, $C_1=\begin{bmatrix}q_{1,min}\\1\\q_{2,min}\end{bmatrix}^T$, $C_2=\begin{bmatrix}q_{1,min}\\1\\q_{2,max}\end{bmatrix}^T$, $C_3=\begin{bmatrix}q_{1,max}\\1\\q_{2,min}\end{bmatrix}^T$ and $C_4=\begin{bmatrix}q_{1,max}\\1\\q_{2,max}\end{bmatrix}^T$. The choice of E_{ai} and E_{si} depend on the input and the output of the battery system. The sensor fault and actuator fault are considered: battery input current and battery terminal voltage which are modeled up to 25% from the rated value for the current and the voltage of the battery. According to the above analysis, the procedure for finding the proposed FFTC controller and the fuzzy adaptive observer for the battery are summarized as follows.

1) Obtain the mathematical model of the battery to be controlled (cf. Section II.C).
2) Obtain the TS fuzzy plant model for the system stated in the previous step by means of a fuzzy modeling method (cf. section III.A.2.d).
3) Solve LMIs (20) and (21) to obtain O, D_i, W_j, H_{bi}, P, L_i, K_i, and G_j thus ($O=P_1^{-1}$, $G_j=W_jO^{-1}$, $\bar{K}_i$=$P_2^{-1}D_i$, $\bar{K}_i=\begin{bmatrix}K_i\\L_i\end{bmatrix}$).

This article has been accepted for publication in a future issue of this journal, but has not been fully edited. Content may change prior to final publication. Citation information: DOI 10.1109/TVT.2018.2805353, IEEE Transactions on Vehicular Technology

4) Construct FFTC controller (19), fuzzy adaptive observer (14) to (18) according to the Theorem 1.

B. Robust Energy Management Controller (Level 2: REMS)

This level is based on [17], its main objective is to manage, optimize and control the power distribution between the two different sources (cf. Figure 7). This level consists of three blocks. The FEMC block splits the required torque between EM or/and HM via ICE (cf. Section III.B.1). The proposed Neural Network Learning Strategy (NNLS) block based on a neural network is used to update FEMC parameters. The Vehicle Global Actual and Suboptimal Efficiency Calculation Algorithm (GASECA) block is used to calculate the total actual and the suboptimal efficiency for the vehicle based on the elementary efficiencies of the EM, battery, ICE, HP, HM and transmission.

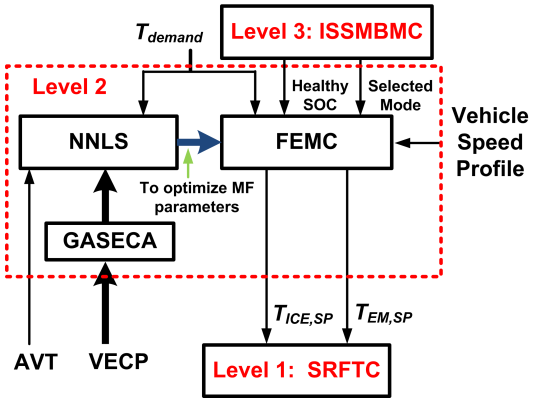

Fig. 7. Block diagram of the proposed level 2.

1) Proposed Fuzzy Energy Management Controller (FEMC): There are three input variables (speed of the vehicle, T_{demand} and SOC) are common for both FSMC and FEMC. In addition, more one input variable (OM) for FEMC. The output variables for FEM are EM torque demand (torque provided by the EM) ($T_{ICE,SP}$) and ICE torque demand (torque provided by the ICE) ($T_{ICE,SP}$). The rules of the proposed fuzzy controller is modified by observing the control surfaces determined by the inputs and outputs. In addition, from the simulation results, the rules of the fuzzy controller can be also modified. Fuzzy rule base for $T_{EM,SP}$ and $T_{ICE,SP}$ in the case of regenerative braking and charging mode are shown in Table II. Where G is the generator (this means the motor works as generator), VA is the very accelerating and A is the accelerating. We design level 2 and level 3 to reduce the number of rules because the input variables are split into two levels (which decrease the rules combination and thus the analysis complexity). The ICE torque (T_{ICE}) and EM torque (T_{EM}) is given as the following, based on FEMC strategy,

$$T_{ICE} = \frac{\sum_{j=1}^{c} m_{ICE,j}\sigma_{ICE,j1}\sigma_{ICE,j2}}{\sum_{j=1}^{c} m_{ICE,j}\sigma_{ICE,j2}} \quad (25)$$

$$T_{EM} = \frac{\sum_{i=1}^{c} m_{EM,i}\sigma_{EM,i1}\sigma_{EM,i2}}{\sum_{i=1}^{c} m_{EM,i}\sigma_{EM,i2}} \quad (26)$$

where, c is the number of fuzzy rules ,where $\sigma_{ICE,j1}$ and $\sigma_{EM,i1}$ are the center of the fuzzy set, $\sigma_{ICE,j2}$ and $\sigma_{EM,i2}$ are width of the fuzzy set of the Gaussian MF, $m_{ICE,j}$ and $m_{EM,i}$ are the inferred weights of the j^{th} and i^{th} output membership function for the ICE and the EM, respectively . The mean and the standard deviation of the output variable are optimized based on the proposed NNLS presented in the following subsection.

TABLE II
FUZZY RULE BASE FOR $T_{EM,SP}$ AND $T_{ICE,SP}$ IN THE CASE OF REGENERATIVE BRAKING AND CHARGING MODE

SOC	T_{demand}	Speed	OM	$T_{EM,SP}$	$T_{ICE,SP}$
L or M	Braking	L or M	RBM	G	zero
L	A	L	CM	G	M
L	A	M	CM	G	H
L	VA	L	CM	G	H

2) Proposed Neural Network Learning Strategy (NNLS): NNLS is developed based on neural networks to optimize the mean and the standard deviation of the FEMC output variable based on the following Theorem 2.

Theorem 2: The parameters required by the FEMC, shown in equations (25) and (26) are updated by the proposed NNLS, if the mean and the standard deviation of the membership function satisfy the following:

$$\sigma_{ij1}^{k+1} = \sigma_{ij1}^{k} - \zeta^{k} \sum_{k=t+1}^{t+s} \sum_{j=1}^{N} \left(e_{ed}^{k} \mu_{td,ij} + e_{eff}^{k} \mu_{eff,ij} \right) \quad (27)$$

$$\sigma_{ij2}^{k+1} = \sigma_{ij2}^{k} - \zeta^{k} \sum_{k=t+1}^{t+s} \sum_{j=1}^{N} \left(e_{ed}^{k} \mu_{td,ij} + e_{eff}^{k} \mu_{eff,ij} \right) \quad (28)$$

where, σ_{ij1} is $\sigma_{ICE,j1}$ and $\sigma_{EM,i1}$ for (25) and (26), and σ_{ij2} is $\sigma_{ICE,j2}$ and $\sigma_{EM,i2}$ for (25) and (26) which are the mean and the standard deviation of the gaussian MF for ICE and the EM, respectively. e_{td} and e_{eff} are the error functions of the torque demand and the vehicle total efficiency, respectively. $\mu_{td,ij}$ and $\mu_{eff,ij}$ are the weights of the i^{th} rule for the j^{th} training pattern, ζ^{k} is the learning rate, k is the iteration index, t is the trailing edge of the moving time-window over which the prediction error is minimized and s is the window of learning. For off-line learning we select $t = 1$ and $s = v$; where v is the size of the training set [49]. The proof of Theorem 2 can be seen in [17].

C. Subsystem Robust Fuzzy Tuning Controllers (Level 1: SRFTC)

Many fuzzy control schemes used in industrial practice today are based on some simplified fuzzy methods, which are simple but at the expense of losing robustness, missing fuzzy characteristics, and having inconsistent inference. In addition, the conventional PID controller is not very efficient due to the presence of non-linearity in the system of the plant and also it has a quite high overshoot and settling time. The concept of fuzzy tuning is introduced in this paper based on based on [50] to overcome these shortcomings. The main objective of

This article has been accepted for publication in a future issue of this journal, but has not been fully edited. Content may change prior to final publication. Citation information: DOI 10.1109/TVT.2018.2805353, IEEE Transactions on Vehicular Technology

this level is to get better dynamic performance at the EM and HM via ICE output.

IV. Simulation Results and Discussion

In order to develop and to evaluate the performance of the proposed overall energy management strategy (called IRHHCS (cf. Section III)), an accurate model of the studied Hybrid Hydraulic-Electric bus is used (cf. Section II). The actual physical HHEV parameters are listed in Table III to VII in Appendix A. In this section, four simulations and discussions to demonstrate the effectiveness of the proposed IRHHCS are presented. The first simulation validate the battery model at low and high temperature during discharging and charging. In the second simulation, the effectiveness of the proposed strategy to detect and compensate the effect of battery faults and its effect on the SOC estimation are presented. The third simulation validates the overall control architecture with battery sensor fault to illustrate the robustness of the proposed technique. The overall proposed control is compared with alternative frameworks existing in the literature based on [10] and [8] in the fourth simulation, in order to demonstrate the advantages of the proposed methodology.

A. Simulation 1: BUSINOVA Battery Model Validation

The objective of this section is to validate the BUSINOVA bus battery model through experimental tests before implementing the diagnostic scheme. BUSINOVA bus battery cell has rated capacity of 80 Ah and nominal voltage of 4.1 V. The simulations have been performed using the equivalent circuit-based model provided in section II.C. Figure 8 (left) shows battery discharging and charging current profiles. Experimental and model output voltage comparison and the voltage error for discharging at high temperature (40^oC) and low temperature (-40^oC) are given in Figure 9 and Figure 10, respectively. Figure 11 shows the comparison of the experimental and model output voltage and the voltage error at high temperature (40^oC) for the pulsating charging current (cf. Figure 8 (right)). Output voltage and the voltage error comparison at low temperature (-40^oC) and constant charging current (80A) is given in Figure 12. Figure 13 and Figure 14 show the comparison of experimental and model output voltages and voltage error at reference temperature (20^oC) and constant charging and discharging current (80A), respectively.

From the simulation results it can be seen that, for low and high temperature the maximum voltage error for discharging and charging are similar to the error found at reference temperature which permit us to conclude that the proposed BUSINOVA battery model is accurate.
From the Figures 9 to 12, one can observe that the proposed model of Lithium-ion battery gives a good modeling performance. For the proposed model, between 10% and 95% SOC, the terminal voltage error around 0.2% which corresponds to lower error compared to voltage error of 1.5% [35].

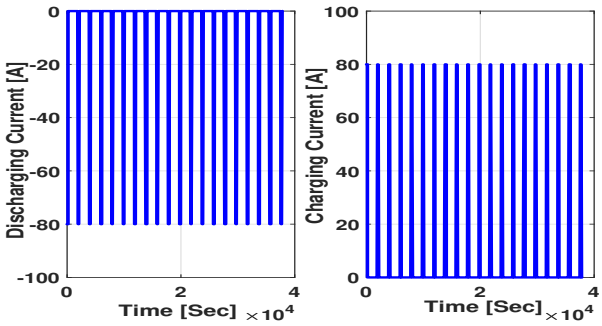

Fig. 8. Battery current profile; (left) battery discharging current profile; (right) battery charging current profile.

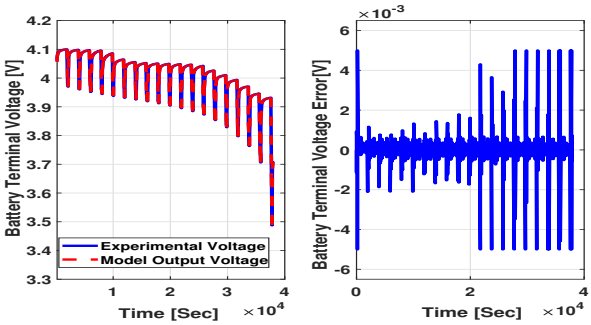

Fig. 9. Comparison of experimental and model output voltages and voltage error at high temperature (40^oC) and discharge current (80A); (left) experimental and model output voltages; (right) voltage error.

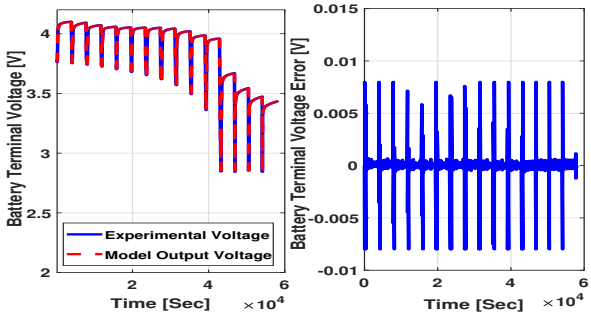

Fig. 10. Comparison of experimental and model output voltages and voltage error at low temperature (-40^oC) and discharge current (80A); (left) experimental and model output voltages; (right) voltage error.

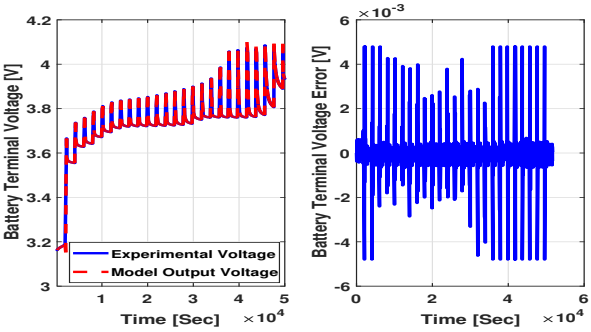

Fig. 11. Comparison of experimental and model output voltages and voltage error at high temperature (40^oC) and charge current (80 A); (left) experimental and model output voltages; (right) voltage error.

This article has been accepted for publication in a future issue of this journal, but has not been fully edited. Content may change prior to final publication. Citation information: DOI 10.1109/TVT.2018.2805353, IEEE Transactions on Vehicular Technology

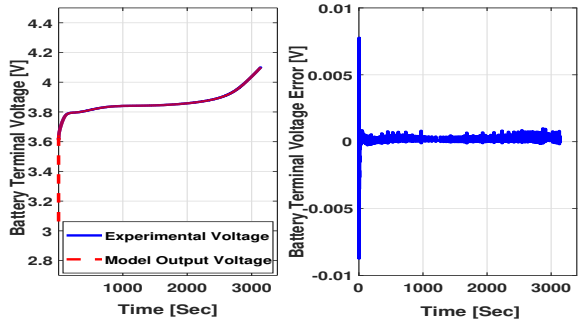

Fig. 12. Comparison of experimental and model output voltages and voltage error at low temperature (-40^oC) and constant charging current (80A); (left) experimental and model output voltages; (right) voltage error.

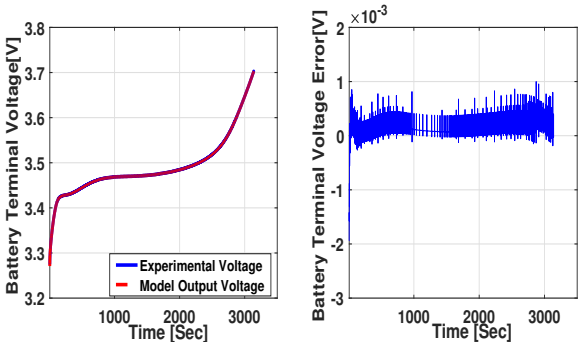

Fig. 13. Comparison of experimental and model output voltages and voltage error for charge at reference temperature (20^oC) and constant charging current (80A); (left) experimental and model output voltages; (right) voltage error.

B. Simulation 2: Fault Detection and its Effects on Battery SOC Estimation

The objective of BMFFTC for the Lithium-ion battery presented in section III.A.2 is to ensure that all signals in the closed-loop battery system are bounded during the battery faults. In this section, the effects of current or voltage sensor faults on the battery SOC estimations and compensation are investigated. For the testing purpose, it is required that sensor and/or actuator fail. The current or voltage sensor faults are injected in the battery test bench. The initial value of the fuzzy observer SOC state is 50%. The tested discharging current profile is given in Figure 15. Figures 16 (left) and (right) show the current sensor fault ($+20$ A bias fault) and voltage sensor fault ($+0.1$ V bias fault) (solid lines) and their estimations (dashed lines) based on the fuzzy observer, respectively. To prevent the battery from over-discharge, the lower limit of the battery SOC is taken as 10%. The current sensor with a ± 20 A bias fault was injected at the time of 2406 sec. Figure 17 (left) plots the experimental SOC estimation under the current sensor fault with FFTC and without FFTC, while Figure 17 (right) shows the SOC estimation errors. It can be found from Figure 17 (left) that the computed SOC in battery management system (observer-estimated SOC) is around 20% at the time of 4812 sec when the current sensor has a $+20$ A bias fault. This induces the battery over-discharge which highly contribute to accelerate the battery aging and thus decrease its life. For a -20 A bias fault, the estimated SOCreaches 10% and the

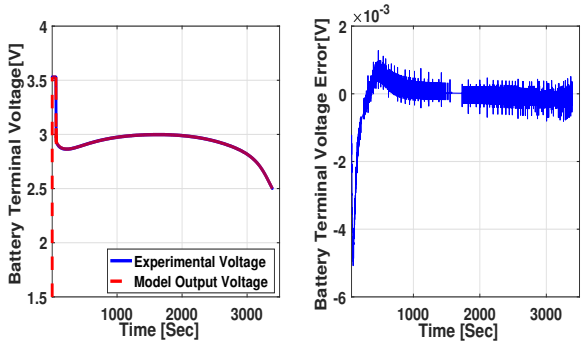

Fig. 14. Comparison of experimental and model output voltages and voltage error for discharge at reference temperature (20^oC) and constant discharging current (80A); (left) experimental and model output voltages; (right) voltage error.

battery cannot release the supposed energy. Also with ± 0.1 V bias fault at the time of 2406 sec, similar simulation results are obtained in Figures 18 (left) and (right). The battery may be over-discharged when the voltage sensor has a $+0.1$ V fault as shown in Figure 18 (left). The estimation errors are up to 22% with the voltage sensor faulty condition (cf. Figure 18 (right)). The results show that the battery may be over-discharged in the faulty sensor cases. The simulation results demonstrate the effectiveness of the proposed control approach. The proposed control scheme can guarantee the stability of the closed-loop battery system. From the simulation results, it can be seen

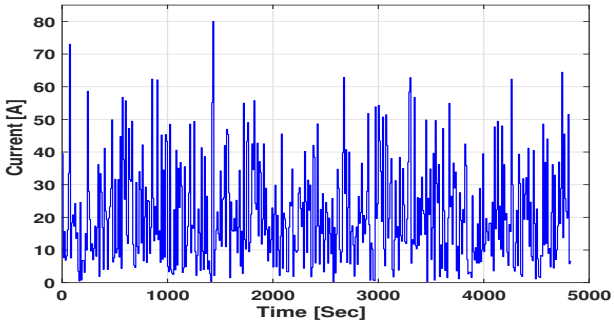

Fig. 15. Battery discharging current profile.

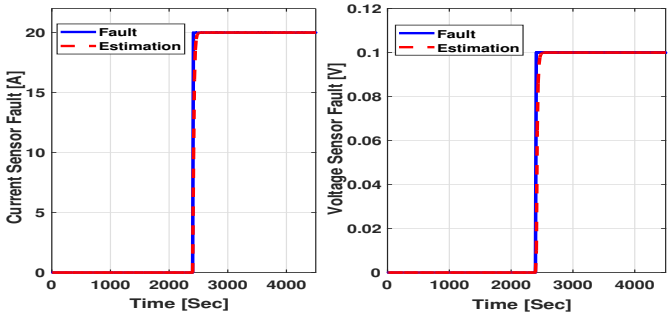

Fig. 16. Battery current and voltage sensor faults and their estimations; (left) battery current sensor fault and its estimation; (right) battery voltage sensor fault and its estimation.

that without the reconfiguration mechanism, the battery lost

This article has been accepted for publication in a future issue of this journal, but has not been fully edited. Content may change prior to final publication. Citation information: DOI 10.1109/TVT.2018.2805353, IEEE Transactions on Vehicular Technology

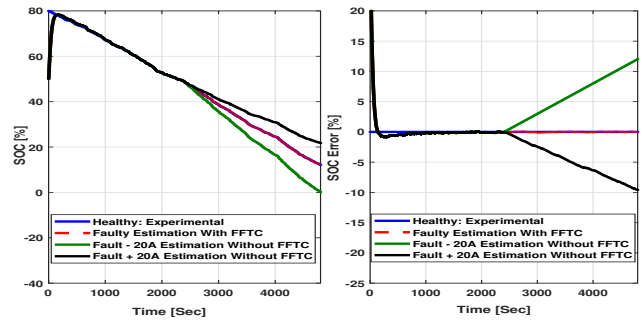

Fig. 17. Effects of current fault on battery SOC estimation; (left) SOC estimation results in the current sensor faulty conditions with and without FFTC; (right) SOC estimation errors in the current sensor faulty conditions with and without FFTC.

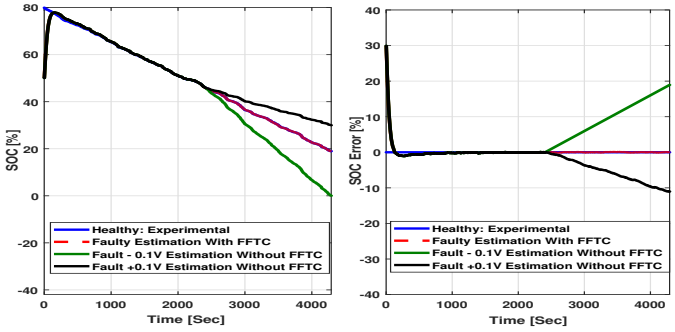

Fig. 18. Effects of voltage fault on battery SOC estimation; (left) SOC estimation results in the voltage sensor faulty conditions with and without FFTC; (right) SOC estimation errors in the voltage sensor faulty conditions with and without FFTC.

performance just after the sensor became faulty, whereas for the same condition and using the proposed FFTC scheme strategy, the battery remains stable in the presence of voltage sensor fault and current actuator fault which demonstrates the effectiveness of the proposed FFTC strategy. In summary, it has been shown that the proposed scheme is able to detect and compensate voltage sensor fault and current actuator fault, through a proper and feasible selection of the observed variables.

C. Simulation 3: Overall Control Architecture Validation with Battery Sensor Fault

The objective here is to show the effectiveness of the proposed overall control architecture (IRHHCS, cf. Section III) to deal with sensor faults. These faults are modeled as an additive signals to battery current sensor output (35% from the nominal current value as bias fault) at the time of 600 sec (cf. Figure 20). In the first simulation the New European Driving Cycles (NEDC) is used (cf. Figure 19). The drive speed profile and output vehicle speed using the proposed strategy with FFTC are shown in Figure 19. The battery SOC trajectory for the proposed strategy with and without FFTC for the same driving cycle is shown in Figure 20. Figure 21 shows the EM energy consumed in [KJ] for the proposed IRHHCS strategy with and without FFTC.

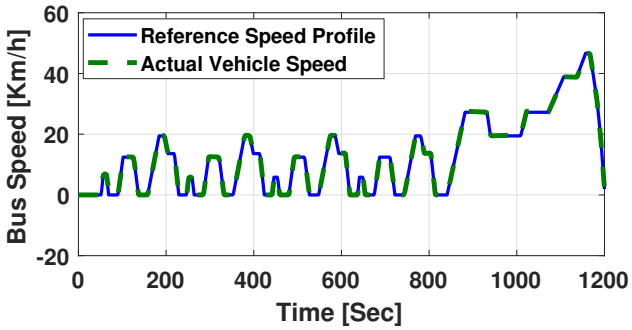

Fig. 19. Vehicle output speed [Km/h] for the proposed strategy over NEDC cycle.

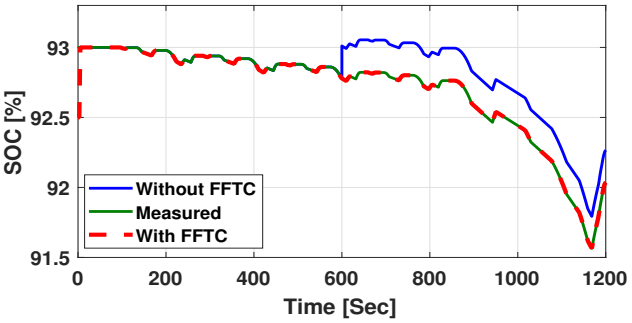

Fig. 20. SOC trajectory for the proposed strategy with and without FFTC over NEDC cycle.

In simulation 2, from the responses of the vehicle subject to current sensor faults, it can be seen that without the FFTC mechanism, the vehicle lost performance and the battery is over-charged just after the sensor became faulty, whereas the vehicle remains stable in the presence of sensor faults. In addition, the consumed energy by EM is small with FFTC compared to the one without FFTC (cf. Figure 21). This demonstrates the effectiveness of the proposed strategy with FFTC.

D. Simulation 4: Comparison Between the Overall Proposed Strategy and Some Alternative Frameworks Existing in the Literature

In this simulation, we compare the results of the proposed algorithm with the previous algorithms HCSF [8] and FBS[10]. This simulation purposes in this paper, the Urban Dynamometer Driving Schedule (UDDS) long cycle, is used to assess the controller performance. The vehicle speed profile and total energy consumed by the vehicle comparison can be seen in Figure 22 and Figure 23, respectively.

By comparing the proposed control strategy and HCSF or FBS, we can see that the total consumed energy has significantly reduced with the proposed IRHHCS. From Figure 23, it can be seen that the total consumed energy of 51809 [KJ] was obtained for the HCSF while the IRHHCS algorithm showed a minimal consumption of 43223 [KJ] and the FBS strategy yielded a fuel consumption of 47115 [KJ].

In summary, it can be seen that the BUSINOVA bus follows the trajectory of the velocity reference input. In addition,

This article has been accepted for publication in a future issue of this journal, but has not been fully edited. Content may change prior to final publication. Citation information: DOI 10.1109/TVT.2018.2805353, IEEE Transactions on Vehicular Technology

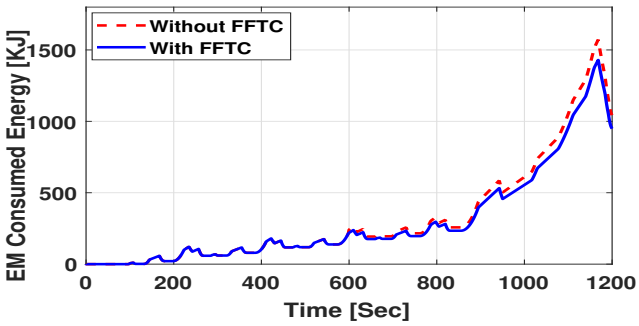

Fig. 21. Energy consumed by the EM in [KJ] for the proposed strategy with and without FFTC over NEDC cycle.

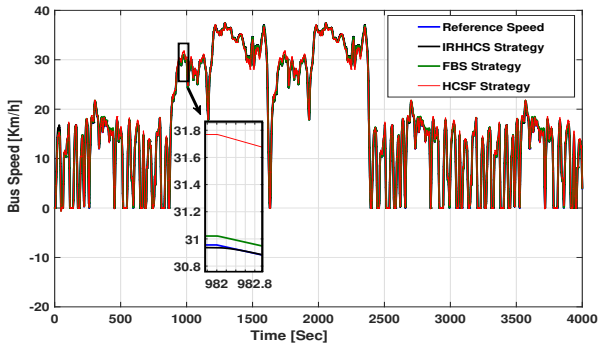

Fig. 22. Drive speed profile and the vehicle speed profile [Km/h] comparison on UDDS between IRHHCS, FBS strategy and HCSF strategy.

the proposed suboptimal energy management architecture is reliable even during current and/or voltage sensor faults (cf. Section IV.B and C).

V. Conclusion

This paper presented a robust energy management strategy, with battery faults detection and compensation for the studied hybrid hydraulic-electric vehicle. The first contribution of the paper is the proposition of an appropriate design of systematic BMFFTC (Battery Management Fuzzy Fault Tolerant Controller) scheme to estimate and compensate the battery faults. Some sufficient conditions for robust stabilization of the TS fuzzy model were derived for a Lithium-ion battery and have been formulated using an LMI (Linear Matrix Inequalities) format. The second contribution of the paper is the reduction of the bus energy consumption while using the proposed Intelligent Robust Hierarchical Hybrid Controller Strategy (IRHHCS). This proposed strategy consists of three control levels. The third level has been developed using fuzzy strategy and fuzzy observer in order: to manage all of the possible bus operation modes and to generate SOC set point for second level and compensate the battery faults. At the second level, an advanced REMS (Robust Energy Management Controller) has been developed for power splitting which decides the suboptimal combination of power sharing (between different energy sources) to minimize the total bus energy consumption while maximizing the overall vehicle efficiency. In the first level, a SRFTC (Subsystem Robust Fuzzy Tuning

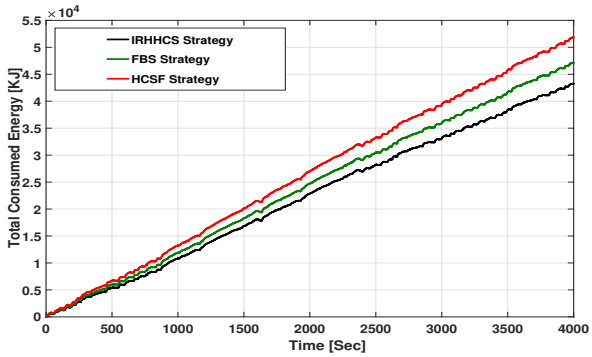

Fig. 23. Total energy consumed by the vehicle in [KJ] comparison on UDDS between IIRHHCS, FBS strategy and HCSF strategy.

Controllers) is defined to get better dynamic performance of the EM and HM via ICE output. Comparing the results of the proposed algorithm with those given by the previous algorithms, it can be noticed that the proposed strategy leads to have several main advantages, among them let us cite: (i) it can be easily implemented in real time and can be used by various structures of hybrid vehicles; (ii) it can reduce, while using appropriate optimization strategy, the total energy consumption (compared to other strategies); (iii) it can detect, isolate and compensate the battery voltage sensor faults and battery current actuator faults; (iv) it does not depend on the a-priori knowledge of the driving event, which making it suitable to be implemented online; (v) it enables to promote the battery longevity while keeping the SOC within a suitable range. Among the main future developments, it is targeted to ensure the robustness of the overall proposed control strategy w.r.t. modelling uncertainties.

VI. Appendix

A. Appendix A

In this appendix, we will present the parameters of the BUSINOVA bus used in IPG automotive TruckMaker software. Where MIRP is Moment of Inertia of the Rotating Parts, RRC is the Rolling Resistance Coefficient, ADC is Air Drag Coefficient, GAC is Gravity Acceleration CE is Combustion Efficiency, DLHV is Diesel Lower Heat Value.

TABLE III
Parameters of the dynamic model of BUSINOVA bus.

Parameter	Value	Parameter	Value
Bus mass [kg]	13490	MIRP [kgm^2]	0.911
RRC	0.009	Wheel radius [m]	0.484
GAC [m/s^2]	9.81	Gear ratio	12.2
Frontal area [m^2]	6.7	Transmission efficiency	0.93
ADC	0.61	Air density [kg/m^3]	1.25

This article has been accepted for publication in a future issue of this journal, but has not been fully edited. Content may change prior to final publication. Citation information: DOI 10.1109/TVT.2018.2805353, IEEE Transactions on Vehicular Technology

TABLE IV
ICE PARAMETERS.

Parameter	Value	Parameter	Value
Max speed, [rpm]	2300	Stroke [m]	0.107
Max torque, [Nm]	343,8 @1400 rpm	C_1 [kPa]	101.5
Max output power [kW]	70.6	DLHV[kJ/kg]	42946
Displacement [mm^3]	82.2	CE	0.75
Diesel density [g/cm^3]	0.8355		

TABLE V
CHARACTERISTICS OF THE HYDRAULIC MOTOR AND PUMP.

Specification	Value	
	Hydraulic motor	Hydraulic pump
Displacement [cm^3]	Variable - [22 - 110]	Fixed - 40
Max torque [Nm]	175 @100 bar	63.5@100 bar
Max speed [rpm]	3400	6100

TABLE VI
PARAMETERS OF THE PERMANENT MAGNET SYNCHRONOUS MOTOR.

Specification	Value	Specification	Value
Nominal speed [RPM]	3240	Nominal current [A]	137
Nominal torque [Nm]	305	Maximum torque [Nm]	660
Nominal power [kW]	103	Maximum speed [RPM]	4000

TABLE VII
MEAN VALUES FOR BUSINOVA BUS BATTERY CELL ELEMENTS.

$R_o[\Omega]$	$R_1[\Omega]$	$C_1[F]$	$R_2[\Omega]$	C_2 [F]	C_n[Ah]
0.0302	0.0124	1.4062e+04	0.0298	7.9338e+03	80

B. Appendix B

This appendix gives the proof for the Theorem 1. In order to carry out the analysis for BMFFTC, the closed-loop fuzzy system should be obtained first by establishing the conditions for the asymptotic convergence of the observers. The fuzzy control system of the state and the errors can be obtained. Substituting (19) into (13), we obtain the dynamics of the closed loop system and the state estimation error:

$$\begin{aligned}&\dot{X}(t) = \textstyle\sum_{i=1}^{p} \mu_i[\bar{A}_i\ X(t))\ + \bar{E}_i f(t)] \\ &+ \textstyle\sum_{i=1}^{p} \mu_i\, \bar{B}_i \left\{ \sum_{j=1}^{p} \mu_j\, [\, G_j\ \hat{X}(t) - E_i \hat{f}(t)] \right\}\end{aligned} \tag{B.1}$$

From (B.1) and (15), we have,

$$\begin{aligned}\dot{X}(t) = &\textstyle\sum_{i=1}^{p} \sum_{j=1}^{p}\ \mu_i\, \mu_j[(\bar{A}_i\ + \bar{B}_i\, G_j]X(t) \\ &+ \textstyle\sum_{i=1}^{p} \mu_i\, \bar{E}_i f(t) - \sum_{i=1}^{p}\ \sum_{j=1}^{p} \mu_i\, \mu_j\, \bar{B}_i\, G_j e_x(t) \\ &- \textstyle\sum_{i=1}^{p} \mu_j\, \bar{B}_i E_i \hat{f}(t)\end{aligned} \tag{B.2}$$

Let

$$\tilde{f}(t) = f(t) - \hat{f}(t) \tag{B.3}$$

From (B.2) and (B.3), a TS fuzzy closed-loop can be observed:

$$\begin{aligned}&\dot{X}(t) = \textstyle\sum_{i=1}^{p}\ \sum_{j=1}^{p}\ \mu_i \mu_j[(\bar{A}_i + \bar{B}_i\, G_j)X(t) \\ &-\bar{B}_i\, G_j\ e_x(t) + \bar{E}_i \tilde{f}(t)]\end{aligned} \tag{B.4}$$

Then taking the derivative of $e_x(t)$ in (15) and substituting from (13), (14) and (B.3), the following is obtained:

$$\dot{e}_x(t) = \sum_{i=1}^{p} [(\bar{A}_i - K_i \bar{C}_i) e_x(t) + \bar{E}_i \tilde{f}(t)] \tag{B.5}$$

The derivative of $\tilde{f}(t)$ in (B.3) can be written as,

$$\begin{aligned}&\dot{\tilde{f}}(t) = \dot{f}(t) - \dot{\hat{f}}(t) = \dot{f}(t) - \textstyle\sum_{i=1}^{p} \mu_i L_i \bar{C}_i \\ &(\textstyle\sum_{i=1}^{p} [(\bar{A}_i - K_i \bar{C}_i + I) e_x(t) + \bar{E}_i \tilde{f}(t)])\end{aligned} \tag{B.6}$$

Combining (B.4), (B.5) and (B.6) yields the following augmented fuzzy system.

$$\begin{aligned}&\dot{\tilde{X}}(t) = \sum_{i=1}^{p} \mu_i \mu_j [\tilde{H}_{ij} \tilde{X}(t) + \tilde{E}_i F(t)] \\ &\tilde{Y}(t) = \sum_{i=1}^{p} \mu_i \tilde{C}_i \tilde{X}(t)\end{aligned} \tag{B.7}$$

with $\tilde{X}(t) = \begin{bmatrix} X(t) \\ e_x(t) \\ \tilde{f}(t) \end{bmatrix}$, $F(t) = \begin{bmatrix} 0 \\ 0 \\ \dot{f}(t) \end{bmatrix}$, $\tilde{E}_i = \begin{bmatrix} 0 & 0 & 0 \\ 0 & 0 & 0 \\ 0 & 0 & I \end{bmatrix}$,
$\tilde{H}_{ij} = \begin{bmatrix} (\bar{A}_i + \bar{B}_i G_j) & -\bar{B}_i G_j) & \bar{E}_i \\ 0 & (\bar{A}_i - K_i \bar{C}_j) & \bar{E}_i \\ 0 & -L_i \bar{C}_i (\bar{A}_i - K_i \bar{C}_i + I) & -L_i \bar{C}_i \bar{E}_i \end{bmatrix}$,
$\tilde{C}_i = \begin{bmatrix} \bar{C}_i & 0 & 0 \end{bmatrix}$, The matrices $\tilde{H}_{ij}$, $\tilde{E}_i$ and $\tilde{C}_i$ can be expressed as:

$$\tilde{H}_{ij} = \begin{bmatrix} (\bar{A}_i + \bar{B}_i G_j) & H_{1ij} \\ 0_{2x1} & H_{2ij} - \bar{K}_i \bar{C}_{1i} \end{bmatrix}, \bar{K}_i = \begin{bmatrix} K_i \\ L_i \end{bmatrix},$$

$$H_{1ij} = \begin{bmatrix} -\bar{B}_i G_j & \bar{E}_i \end{bmatrix}, \tilde{C}_i = \begin{bmatrix} \bar{C}_i \\ 0 \end{bmatrix}^T, \tilde{E}_i = \begin{bmatrix} 0 & 0 \\ 0 & I \end{bmatrix},$$

$$H_{2ij} = \begin{bmatrix} \bar{A}_i & \bar{E}_i \\ -L_i \bar{C}_i (\bar{A}_i - K_i \bar{C}_i) & -L_i \bar{C}_i \bar{E}_i \end{bmatrix}.$$

Let us consider the following quadratic Lyapunov candidate function $V(t)$:

$$V(t) = \tilde{X}(t)^T P \tilde{X}(t) \tag{B.8}$$

where P is common positive definite matrix. The problem of robust state and fault estimation is to find the gains G_j, K_i and L_i of the controller and the observers to ensure an asymptotic convergence of $X(t)$ toward zero when $F(t) = 0$. This problem is reduced to find P verifying $\dot{V}(t) < 0$, i.e.,

$$\dot{\tilde{X}}(t) = \sum_{i=1}^{p} \mu_i\, \tilde{H}_i\, \tilde{X}(t) \tag{B.9}$$

By the derivative time of $V(t)$ and substituting (B.9), one obtain

$$\dot{V}(t) = \frac{1}{2} \tilde{X}(t)^T \sum_{i=1}^{p} \mu_i (\tilde{H}_i^T P + P \tilde{H}_i) \tilde{X}(t) \tag{B.10}$$

From (B.10), the derivative time of (B.8) is uniformly negative if the following inequality is satisfied

$$P \tilde{H}_{ij} + \tilde{H}_{ij}\ ^T P < 0 \qquad \forall i, j \tag{B.11}$$

Let $P = \begin{bmatrix} P_1 & 0 \\ 0 & P_2 \end{bmatrix}$, Therefore, the inequality (B.11) will be rewritten as:

$$P_1(A_i - B_i G_j) + (A_i - B_i G_j)^T P_1 < 0 \quad \forall i, j \tag{B.12}$$

$$P_2(H_{bi}-\bar{K}_i\bar{C}_i)+(H_{bi}-\bar{K}_i\bar{C}_i)^T P_2 < 0 \quad \forall i,j \qquad (B.13)$$

By multiplying (B.12) from left and right by $O = P_1^{-1}$, and applying the change of variables $O = P_1^{-1}$, $W_j = G_j O$, $D_i = P_2\bar{K}_i$, LMIs (20) and (21) are obtained.

REFERENCES

[1] J. M. German, Hybrid powered vehicles, Society of Automotive Engineers (SAE) publication T-119, 2003.

[2] A. Panday and H. O. Bansal, Energy Management Strategy Implementation for Hybrid Electric Vehicles Using Genetic Algorithm Tuned Pontryagin's Minimum Principle Controller, International Journal of Vehicular Technology, vol. 2016, pp.1-13, 2016.

[3] R. Abdrakhmanov and L. Adouane, Dynamic Programming Resolution and Database Knowledge for Online Predictive Energy Management of Hybrid Vehicles, International Conference on Informatics in Control, Automation and Robotics (ICINCO), 26-28 July, Madrid-Spain.

[4] L. Johannesson, M. Asbogard and B. Egardt, Assessing the potential of predictive control for hybrid vehicle powertrains using stochastic dynamic programming, Transactions ITSC, vol. 8, no. 1, 2007, pp. 71-83, 2007.

[5] S. J. Moura, H. K. Fathy, D. S. Callaway and J. L. Stein, A stochastic optimal control approach for power management in plug-in hybrid electric vehicles, IEEE Transactions on Control Systems Technology, vol. 19, no. 3, pp. 545-555, 2011.

[6] N. Ouddah, L. Adouane, R. Abdrakhmanov and E. Kamal, Optimal Energy Management Strategy of Plug-in Hybrid Electric Bus in Urban Conditions, International Conference on Informatics in Control, Automation and Robotics (ICINCO), 26-28 July, Madrid-Spain.

[7] X. C. Ying and Z. Cong, Real-time optimization power-split strategy for hybrid electric vehicles, Sci China Tech Sci, vol. 59, no. 5, pp. 814- 824, 2016.

[8] B. Adel, Z. Youtong and S. Shua, Parallel HEV Hybrid Controller Modeling for Power Management,World Electric Vehicle Journal, vol. 4 - ISSN 2032-6653, pp. 190-196, 2010.

[9] Y. Lihao, W. Youjun and Z. Congmin, Study on Fuzzy Energy Management Strategy of Parallel Hybrid Vehicle Based on Quantum PSO Algorithm, International Journal of Multimedia and Ubiquitous Engineering, vol. 11, no. 5, pp. 147-158, 2016.

[10] N. Denis, M. R. Dubois and A. Desrochers, Fuzzy-based blended control for the energy management of a parallel plug-in hybrid electric vehicle, IET Intelligent Transport Systems, vol. 9, no.1, pp. 30 -37, 2015.

[11] D. Y. Wang, X. Lin, Y. Zhang, Fuzzy logic control for a parallel hybrid hydraulic excavator using genetic algorithm, Automation in Construction, vol. 20, no. 5, pp. 581-587, 2011.

[12] Y.-C. Chiou, L. W. Lan, Genetic fuzzy logic controller: an iterative evolution algorithm with new encoding method, Fuzzy Sets and Systems, vol. 152, no. 3, pp. 617-635, 2005.

[13] C. Marina Martnez, X.Hu, D. Cao, E. Velenis, B. Gao and M. Weller, Energy Management in Plug-in Hybrid Electric Vehicles: Recent Progress and a Connected Vehicles Perspective, IEEE Transactions on Vehicular Technology, vol. 66, no. 6, pp. 4534- 4549, 2017.

[14] N. R. Cazarez-Castro, L. T. Aguilar, O. Castillo, Fuzzy logic control with genetic membership function parameters optimization for the output regulation of a servomechanism with nonlinear backlash. Expert Systems with Applications, vol. 37, no. 6, pp. 4368- 4378, 2010.

[15] K. Yang, J. Zheng, M. Yang, R. Zhou, G. Liu, Adaptive genetic algorithm for daily optimal operation of cascade reservoirs and its improvement strategy, Water Resources Management, vol. 27, no. 12, pp. 4209-4235, 2013.

[16] X. Dai, C. K. Li, and A. B. Rad, An Approach to Tune Fuzzy Controllers Based on Reinforcement Learning for Autonomous Vehicle Control, IEEE Transactions on Intelligent Transportation Systems, vol. 6, no. 3, pp. 285-293, 2005.

[17] E. Kamal and L. Adouane, Intelligent Energy Management Strategy based on Artificial Neural Fuzzy for Hybrid Vehicle, IEEE Transactions on Intelligent Vehicles, vol. 3, no. 1, 2018.

[18] M. L. Zhou, D. K. Lu, W. M. Li and H. F. Xu, Optimized Fuzzy Logic Control Strategy for Parallel Hybrid Electric Vehicle Based on Genetic Algorithm, Appl. Mech. Mater, vol. 274, pp. 345-349, 2013.

[19] E. S. Rigas, S.D. Ramchurn, and N. Bassiliades, Managing Electric Vehicles In the Smart Grid Using Artificial Intelligence: A Survey, IEEE Transactions on Intelligent Transportation Systems, vol. 16, no. 4, pp. 1619-1635, 2015.

[20] J. Klee Barillas, J. Li, C. Gnther and M. Danzer, A comparative study and validation of state estimation algorithms for Li-ion batteries in battery management systems. Appl Energy, vol.155, pp.455-462, 2015.

[21] L. Lu, X. Han, J. Li, J. Hua and M. Ouyang, A review on the key issues for lithium-ion battery management in electric vehicles. J Power Sources, vol. 226, pp. 272-288, 2013.

[22] L. Zhentong and H. Hongwen, Sensor fault detection and isolation for a lithium-ion battery pack in electric vehicles using adaptive extended Kalman filter, Applied Energy, vol. 185, pp. 2033-2044, 2017.

[23] S. Dey, S. Mohon, P. Pisu and B. Ayalew, Sensor fault detection, isolation, and estimation in Lithium-ion batteries, IEEE Transactions on Control Systems Technology, vol. 24, no. 6, pp. 2141-2149, 2016.

[24] Z. Liu, Q. Ahmed, J. Zhang, G. Rizzoni and H. He, Structural analysis based sensors fault detection and isolation of cylindrical lithium-ion batteries in automotive applications, Control Engineering Practice, vol. 52, pp.46-58, 2016.

[25] Z. Liu, Q. Ahmed, G. Rizzoni and H. He, Fault detection and isolation for lithium-ion battery system using structural analysis and sequential residual generation, ASME dyn. syst. control conf. pp. 110, 2014.

[26] A. Sidhu, A. Izadian and S. Anwar, Model-Based Adaptive Fault Diagnosis in Lithium Ion Batteries: A Comparison of Linear and Nonlinear Approaches, SAE Technical Paper 2017-01-1192, 2017.

[27] A. Sidhu, A. Izadian and S. Anwar, Adaptive Nonlinear Model-Based Fault Diagnosis of Li-ion Batteries, IEEE Transaction on industrial Electronics, vol. 26, no. 2, pp. 1002-1010, 2015.

[28] L. Seybold, M. Witczak and P. Majdzik, Predictive fault-tolerant control for a battery assembly system, IFAC (International Federation of Automatic Control), PapersOnLine 48-21, pp. 476-483, 2015.

[29] M. Chen and G. A. Rincon-Mora, Accurate Electrical Battery Model Capable of Predicting Runtime and I-V Performance, IEEE Transactions on Energy Conversion, vol. 21, no. 2, pp. 504-511, 2006.

[30] J. Jaguemont, L. Boulon and Y. Dub, Characterization and Modeling of a Hybrid-Electric-Vehicle Lithium-Ion Battery Pack at Low Temperatures, IEEE Transactions on Vehicular Technology, vol. 65, no. 1, pp. 1-14, 2016.

[31] T. Mesbahi, F.Khenfri, N. Rizoug and K.Chaaban, P. Bartholomes and P. Le Moigne, Dynamical modeling of Li-ion batteries for electric vehicle applications based on hybrid Particle Swarm-Nelder-Mead (PSO-NM) optimization algorithm, Electric Power Systems Research, vol. 131, pp. 195-204, 2016.

[32] H. He, R. Xiong, H. Guo and S. Li, Comparison study on the battery models used for the energy management of batteries in electric vehicles, Energy Convers. Manag., vol. 64, pp.113-121, 2012.

[33] X. Hua, S. Li and H. Peng, A comparative study of equivalent circuit models for Li-ion batteries, Journal of Power Sources, vol. 198, pp. 359-367, 2012.

[34] D. Dvorak, H. Lacher and D. Simic, Thermal Modeling and Validation of a Lithium-Ion Battery Based on Electric Vehicle Measurements, IEEE Vehicle Power and Propulsion Conference (VPPC), Oct. 27-30, 2014.

[35] S. Sepasi, R. Ghorbani and B.Y. Liaw, Improved extended Kalman filter for state of charge estimation of battery pack, Journal of Power Sources, vol. 255, no.1, pp. 368-376, 2014.

[36] E. Kamal, A. El Hajjaji and A. M. Mabwe, State of Charge Estimation Based on Extended Kalman Filter Algorithm for Lithium-ion Battery, 23rd Mediterranean Conference on Control and Automation, 16-19 June, Torremolinos-Spain, 2015.

[37] E. Kamal, A. El Hajjaji and A. Mpanda Mabwe, Dynamic Model Parameters identification for Lithium-Ion Batteries, 2015 IEEE Multi-Conference on Systems and Control (MSC), 21-23 Sep., Sydney-Australia, , 2015.

[38] S. Mohan, Y. Kim and A. G. Stefanopoulou, Estimating the Power Capability of Li-ion Batteries Using Informationally Partitioned Estimators, IEEE Transactions on Control Systems Technology, vol. 24, no. 5, pp. 1643-1654, 2016.

[39] S. Mohan, Y. Kim and A.G. Stefanopoulou, Estimating the Power Capability of Li-ion Batteries Using Informationally Partitioned Estimators, IEEE Transactions on Control Systems Technology, vol. 24, no. 5, pp. 1643-1654, 2016.

[40] F. Xu, X. Jiao, M. Sasaki and Y. Wang, Energy management optimization in consideration of battery deterioration for commuter plug-in hybrid electric vehicle, 55th Annual Conference of the Society of Instrument and Control Engineers of Japan (SICE), pp. 218-222, 2016.

[41] L. Tang, G. Rizzoni, and S. Simona, Energy Management Strategy for HEVs Including Battery Life Optimization. IEEE Transactions on Transportation Electrification, vol. 1, pp. 1-10, 2015.

[42] T. M. Padovani, M. Debert, G.Colin and Y. Chamaillard, Optimal Energy Management Strategy Including Battery Health through Thermal

Management for Hybrid Vehicles, IFAC Proceedings Volumes (IFAC-PapersOnline), vol.7, 2013
[43] X. Hu, C. M. Martinez and Y. Yang, Charging, power management and battery degradation mitigation in plug-in hybrid electric vehicles: A unified cost-optimal approach, Mechanical Systems and Signal Processing, 2016.
[44] E. Kamal and A. Aitouche, Robust Scheduler Fuzzy Controller of DFIG Wind Energy Systems, IEEE Transactions on Sustainable Energy, vol. 4, no 3, pp. 706-715, 2013.
[45] E. Balaban, A. Saxena, P. Bansal, K.F. Goebel and S. Curran, Modeling, Detection, and Disambiguation of Sensor Faults for Aerospace Applications. IEEE Sens. J., vol. 9, pp. 1907-1917, 2009.
[46] G. H. Foo, X. Zhang and D. M. Vilathgamuwa, A Sensor Fault Detection and Isolation Method In Interior Permanent-Magnet Synchronous Motor Drives Based on an Extended Kalman Filter. IEEE Trans. Ind. Electron., vol. 60, pp. 3485-3495, 2013.
[47] C. Edwards, A Comparison of Sliding Mode and Unknown Input Observers for Fault Reconstruction, European journal of control, vol.12, no.3, pp. 245-260, 2006.
[48] E. Kamal, A. Aitouche, R. Ghorbani and M. Bayart, Robust Fuzzy Fault Tolerant Control of Wind Energy Conversion Systems Subject to Sensor Faults, IEEE Transactions on Sustainable Energy, vol. 3, no 2, pp. 231-241, 2012.
[49] L. Ljung, System identification: theory for the users, (2nd ed.) Upper Saddle River, NJ: Prentice-Hall,1999.
[50] B. Hamed and M. Almobaied, Fuzzy PID Controllers Using FPGA Technique for Real Time DC Motor Speed Control, Intelligent Control and Automation, vol. 2, pp. 233-240, 2011.
[51] O. H. Rodrguez and J. M. L. Fernndez, A Semiotic Reflection on the Didactics of the Chain Rule, The Montana Mathematics Enthusiastl, vol. 7, pp. 321-332, 2010.
[52] A.-K. Jain, R. C. Dubes, Algorithms for Clustering Data, Prentice Hall, Englewood Cliffs, NJ, 1988.

Elkhatib Kamal is an Assistant Professor since 2015 at the Department of Industrial Electronics and Control Engineering, Faculty of Electronic Engineering in Menouf, Menoufia University in Egypt. He received the B.Sc. and M.Sc. degrees from the Faculty of Electronic Engineering, Menoufia University, Shebin EL Kom, Egypt, in 2002 and 2007, respectively, and the Ph.D. degree from the Laboratoire de recherche CRIStAL UMR 9189: Centre de Recherche en Informatique, Signal et Automatique de Lille, Université des Sciences et Technologies de Lille, France, in 2013. He is a Researcher with Institut Pascal / Innovative Mobility: Smart and Sustainable Solutions (IMobS3), UCA/SIGMA UMR CNRS 6602, Clermont-Ferrand, France. His current research interests include analysis and design of intelligent control systems such as fuzzy control, neuro fuzzy control, robust control, fault-tolerant systems, fault-tolerant control, model-based fault detection and diagnosis, energy management and battery life cycle analysis for electric mobility with their applications in transportation, process engineering, renewable energy and hybrid vehicle. He has published several publications in these areas.

Lounis Adouane is an Associate Professor since 2006 at the Institut Pascal Polytech Clermont-Ferrand in France. He received an MSc in 2001 from IRCCyN-ECN, Nantes, where he worked on the control of underactuated legged robot. In 2005, he obtained a Ph.D. in automatic control from FEMTO-ST laboratory-UFC Besancon. During his Ph.D. studies he deeply investigated the field of complex multi-robot systems, especially those related to bottom-up control architectures. After that, he joined in 2005 Ampere laboratory-INSA Lyon and studied hybrid (continuous/discrete) control architectures applied to cooperative mobile robot arms. In 2015, he obtained from Blaise Pascal University a HDR (habilitation to steer research in Robotics). Since 2006, he has authored/coauthored more than 80 international references and 2 books. His main research interests include: Autonomous and clean vehicles, Hybrid Electric Vehicles, Energy management strategy, Behavioral/multi-controller architectures, Optimal and Artificial Intelligence based control, Lyapunov-based synthesis and stability.